Knowledge-based structural models of SARS-CoV-2 proteins and their complex with potential drugs

Atsushi Hijikata[1], Clara Shionyu-Mitsuyama[1], Setsu Nakae[1], Masafumi Shionyu[1], Motonori Ota[2], Shigehiko Kanaya[3], and Tsuyoshi Shirai[1,*]

[1]Faculty of Bioscience, Nagahama Institute of Bio-Science and Technology, 1266, Tamura-cho, Nagahama, Shiga, 526-0829, Japan

[2]Department of Complex Systems Science, Graduate School of Informatics, Nagoya University, Furo-cho, Chikusa-ku, Nagoya, Aichi 464-8601, Japan

[3]Computational Biology Lab. Division of Information Science, Graduate School of Science and Technology, Nara Institute of Science and Technology (NAIST), 8916-5, Takayama-cho Ikoma, Nara, 630-0192, Japan

[*]Correspondence: t_shirai@nagahama-i-bio.ac.jp

ABSTRACT

The World Health Organization (WHO) has declared a pandemic of the 2019 novel coronavirus SARS-CoV-2 infection (COVID-19). There is, however, no confirmed anti-COVID-19 therapeutic currently. In order to assist structure-based discovery of repurposing drugs against this disease, knowledge-based models of SARS-CoV-2 proteins were constructed, and the ligand molecules in the template structures were compared with approved/experimental drugs and components of natural medicines. The models suggested several drugs, such as carfilzomib, sinefungin, tecadenoson, and trabodenoson, as potential drugs for COVID-19.

INTRODUCTION

The newly identified coronavirus (SARS-CoV-2) was found to cause severe pneumonia (COVID-19), and rapidly spread across the world from the initial outbreak point in Wuhan, China in late 2019[1, 2]. It became a global health emergency, and the World Health Organization (WHO) has declared a pandemic status of this novel coronavirus outbreak in Mar 11th 2020. Since no approved drug that is specifically targeted to this virus exists at this point of time, drug repositioning/repurposing is thought to be the most effective and feasible approach toward this clear and present threat, and the researchers have initiated studies by employing various means in order to found potential therapeutics [3-11].

SARS-CoV-2 genome was very close to that of the severe acute respiratory syndrome coronavirus (SARS-CoV) [1, 2]. From the past efforts to cure RNA-virus infections, including the experiences from the SARS and Middle East Respiratory Syndrome (MERS) epidemics, several potential target proteins and drugs have been proposed [12, 13]. The 3C-like (main) proteinase, surface glycoprotein [8], and RNA-dependent RNA polymerase are thought to be the most promising targets for anti-COVID-19 therapeutics. For example, the anti-HIV drug lopinavir/ritonavir, which have been proposed to treat SARS [14, 15], is expected to be effective toward SARS-CoV-2 3C-like proteinase [16-18]. Additionally, the anti-viral drug remdesivir is expected to target the RNA-dependent RNA polymerase [19].

The studies of recent drug repositioning/repurposing involve a variety of computational methods, such as network analysis, text mining, machine learning, and structural-based drug repositioning (SBDR) [20-25]. Among these methods, SBDR is most promising to find specific drugs toward a defined target protein, and it prompted the quick structure analyses of SARS-CoV-2 3C-like proteinase and surface glycoprotein [8, 26].

Although structure analyses of many other SARS-CoV-2 proteins would soon follow, predictions of other protein structures with homology/knowledge-based (theoretical) methods would be required until structure analyses are completed, especially for the proteins currently out of focus as drug-targets. In the presented study, therefore, the homology models of SARS-CoV-2 proteins and their ligand complexes

were comprehensively constructed. Also, the structural models of the complex between SARS-CoV-2 proteins and potential drugs were proposed by comparing the ligand molecules of the proteins and the approved, experimental, or natural drugs.

MATERIALS AND METHODS

Homology modeling of SARS-CoV-2 proteins

The amino acid sequences of SARS-CoV-2 proteins (Table1) were retrieved from the Refseq database at NCBI [27], and structural modeling templates were sought with the SIRD system (http://sird.nagahama-i-bio.ac.jp/sird/), which accepted multiple-query sequences and sought for similar sequences (more than 30% sequence identity to query) with known-structures in the Protein Data Bank (PDB) [28] by using BLAST [29]. This system also sought for the templates of protein complex structures, in which two or more proteins in the multiple-query were associated or any ligand bound to query proteins. The coordinates of template structures were obtained from the PDB [28], and were rendered into the biological quaternary structures.

Initial structural models were constructed by using MODELLER [30]. The models were further refined by iteratively applying molecular dynamics and geometry minimization procedures of PHENIX [31], and manual model modifications on COOT [32]. The model quality was evaluated with MolProbity [33]. The percentages of rotamer outlier, Ramachandran outlier, and crash score were monitored for each model to achieve less than 2%, 0.05%, and 5, respectively.

Modeling of SARS-CoV-2 protein complexes with potential drugs

The molecular formula of 8,085 drugs in total were retrieved from KEGG database [34] and DrugBank database [35]. The molecular formula of 5,780 metabolites in total, which have been used for natural medicines (natural drugs) were obtained from KNApSAcK database [36].

The structures of the ligand molecules in the known complex structures, as sought in the template-search process, were exhaustively compared with that of the drugs by using COMPLIG [37]. COMPLIG matches molecular graphs, and evaluates the similarity score of two molecules A and B as $\min\{M(A, B)/M(A), M(A, B)/M(B)\}$, where $M(A)$ and $M(B)$ are the total numbers of atoms and bonds in molecules A and B, respectively, and $M(A, B)$ is the total number of atoms and bonds matched between molecules A and B. Both element and chirality, if applicable, should be identical for atoms, and bond order should be identical for bonds to be matched.

Selected drug molecules were built into the protein models by superposing drug molecules to known (original) ligand molecules with COMPLIG. According to the graph matching results, the dihedral angles in the drug molecules were adjusted toward the corresponding angles in the original ligand molecules, and corresponding atoms were superposed between drug and known ligand by fixing the coordinates of the latter. The models of protein - drug complexes were further refined with PHENIX and COOT. The constraints for drug molecules were generated by using the eLBOW application in PHENIX.

RESULTS

Models of SARS-CoV-2 protein

The SARS-CoV-2 genome encodes 11 genes (open reading frames), and the polyprotein from orf1ab is processed into 16 proteins (polypeptides) through cleavages by the papain-like proteinase and 3C-like proteinase activities [1, 12, 38]. As a result of template search, the appropriate structural templates were found for 17 SARS-CoV-2 proteins among a total of 26, and their homology models were constructed (Table 1). The 9 unmodeled proteins included those from very short ORFs, namely, Nsp11 (13 amino acid residues), ORF7b (43 residues), and ORF10 (38 residues) and probable membrane proteins (nsp6, ORF3a, ORF6, M, and ORF8), which were annotated by the SOSUI server [39].

Since a considerable amount of structural studies have already done for SARS-CoV and MERS-CoV proteins, most of the available templates were from these viruses, and they had high-sequence similarity (more than 90%) to SARS-CoV-2 proteins. Two proteins, namely, papain-like proteinase (nsp3) and nucleocapsid phosphoprotein could not be modeled into a single structural model, and separated into 6 and 2 fragments, respectively. As a consequence, the coverage of structural model was lowest (56% of residues) for papain-like proteinase (nsp3).

Third region of papain-like proteinase (nsp3), nsp4, 3C-like proteinase, nsp9, endo-RNAse, surface glycoprotein, envelope protein, and C-terminal region of nucleocapsid phosphoprotein were modeled into homo-multimer. As the

6

hetero-multimeric models, nsp7 and nsp8 were modeled into hetero-16mer, RNA-dependent RNA polymerase, nsp7, and nsp8 were modeled as hetero-tetramer (1:1:2 stoichiometry), 3'-to-5' exonuclease and nsp10 formed hetero-dimer, 2'-O-ribose methyltransferase and nsp10 also formed hetero-dimer, and homo-trimer of surface glycoprotein was modeled in complex with human angiotensin I converting enzyme 2 (ACE2) (Table 1).

Models of SARS-CoV-2 protein with drug

Although the models of SARS-CoV-2 protein would be useful for structure-based virtual screening, potential drugs for these proteins were sought by rather simple knowledge-based method in the presented study. The ligand molecules that were complexed with the homologs of SARS-CoV-2 protein in the PDB were extracted, and structurally similar molecules to the ligands were sought among the approved/experimental drugs retrieved from KEGG database [34] and DrugBank database [35]. Many of the approved drugs, such as morphine, aspirin, or penicillin, have been adapted from natural medicines [40, 41]. The molecules in the natural medicines are expected to serve as argent therapeutics. Therefore, the ligand structures were also compared with the components of natural medicines (natural drugs) registered in the KNApSAcK database [36].

The original ligand molecules and the detected drug molecules were summarized in Table 2. A total of 11 ligand molecules were matched to 21 approved/experimental and 5 natural drugs, and the complex models of the SARS-CoV-2 proteins with several

promising drugs, those with high similarity score or placed in higher ranking, were constructed as follows.

3C-like proteinase

3C-like proteinase is involved in the processing of viral polyprotein [42]. This enzyme is one of the most extensively studied drug target, and thus analyzed in complex with various peptide-mimetic inhibitors [43-46]. Unexpectedly, these ligands did not show very high similarity to known drug molecules (Table 2). As a peptide mimetic drug, carfilzomib showed highest score to the template ligand (ligand code AZP) of 3C-like proteinase homolog (Fig. 1A). However, the similarity score between the ligand and the drug was only 0.754. Carfilzomib is the irreversible proteasome inhibitor targeted to the subunits with chymotrypsin-like activity and has been approved for refractory multiple myeloma or Waldenström's macroglobulinemia [47, 48]. A complex model of carfilzomib - SARS-CoV-2 3C-like proteinase was constructed. In the model, carfilzomib formed a parallel β-sheet with His164 – Glu166, and side chains of His41, Cys145, Met165, Leu167, Phe185, and Gln189 contributed major interactions (Figs. 1B and 1C). These residues were conserved between the template (SARS-CoV) and the model (SARS-CoV-2) proteins. Carfilzomib covalently binds to active site threonine through epoxy moiety, and the epoxy moiety is also reactive with thiol group of cysteine [47, 49]. Although a possible covalent linkage between carfilzomib and the catalytic Cys145 of SARS-CoV-2 3C-like proteinase was not explicitly modeled, the epoxy moiety was placed close to the catalytic residue in this model.

Surface glycoprotein-ACE2 complex

Surface glycoprotein is used for a viral entrance into the host cell, and its cell-surface receptor is human angiotensin I-converting enzyme 2 (ACE2) [50]. ACE, a homolog of ACE2 sharing 44% amino acid sequence identity, is a major target of hypertension medicating drugs, and several ACE-drug complexes have been reported [51-53]. Lisinopril, enalaprilat, and captopril, which show similar structures to each other (Fig. 2A), have been targeted toward ACE, and approved for hypertension treatments [54-57]. In the structural complex models, these drugs were bound to the protein through a Zn^{2+}-coordination with Glu384, His356, and His360 (Figs. 2B and 2C). These residues were conserved between the template (ACE) and the model (ACE2) structures. Although the drug molecules also formed electrostatic interactions with Arg255 and Arg500, these residues were not conserved between ACE and ACE2. The SARS-CoV-2 surface glycoprotein interacted with ACE2 through the receptor-binding domain (RBD), while the bound drugs had no direct interaction to the RBD domain (Fig. 2C).

2'-O-Ribose methyltransferase

The complex of 2'-*O*-ribose methyltransferase (nsp16) and nsp10 is involved in the modification of the viral RNA caps [58]. The structure of 2'-*O*-ribose methyltransferase subunit was determined in complex with S-adenosyl-L-methionine (ligand code SAM), 7-methyl-guanosine-5'-triphosphate- 5'-guanosine (GTG), and sinefungin (SFG) [59-61]. Among these ligands, S-adenosyl-L-methionine is used for a therapeutic against

9

depression, liver disorders, fibromyalgia, and osteoarthritis [62], but also is an authentic substrate for this enzyme. Sinefungin is a natural drug produced by *Streptomyces griseolus*, and experimentally used as antibiotics [63-65] (Fig. 3A).

The residues of 2'-*O*-ribose methyltransferase, Ser74, Asp99, Asn101, Asp130, and Met131, were involved in the major interactions with sinefungin (Figs. 3B and 3C). These residues were conserved among the template proteins (SARS-CoV and betacoronavirus) and SARS-CoV-2.

As the drugs similar to these ligands, several investigational adenosine A1 receptor agonists, namely, tecadenoson, selodenoson, trabodenoson, were found (Fig. 3A). These molecules share adenosine moiety, and this moiety interact with the aforementioned 5 conserved residues in the complex models.

DISCUSSION

In the presented study, the knowledge-based models of SARS-CoV-2 proteins were constructed by homology modeling and comparison of the known ligands with drugs. Since a considerable number of structure analyses have already reported for coronavirus proteins including those of SARS-CoV, 66% (17/26) of the SARS-CoV-2 proteins could be modeled based on highly similar (85% sequence identity and 89% coverage on average) templates (Table 1).

Several drugs were suggested to bind to the SARS-CoV-2 targets (Table 2). The procedure employed in the presented study should largely limit the extent of search (because depend on the presence of ligands in known complex structures). However, it

10

is noteworthy that the binding of suggested drugs to the homologous proteins of the SARS-CoV-2 targets would be probable because of the presence of structural evidences.

The complex models were constructed for several high-scored and/or high-ranked drugs. Unexpectedly, no drug was detected for one of the most promising drug targets, 3C-like proteinase, with a similarity score higher than 0.8. In the previous study, the score more than 0.8 was suggested to be required for highly similar interactions between ligand and protein [37]. It implied that the inhibitors bound to the 3C-like proteinase in the known structures are considerably deviated from most of the approved protease-targeted drugs. For example, the anti-HIV drug lopinavir/ritonavir, which was expected to target SARS-CoV-2 3C-like proteinase [16-18], showed only limited similarity (score 0.513) to the known ligand (ligand code AXP) of SARS-CoV 3C-like proteinase (Fig. 2A). One possible reason of the low similarity to drugs is that the protease inhibitors tend to have higher-molecular weight and thus their molecular structures showed large variety. Another reason would be that a majority of the protease inhibitory drugs are targeted toward serine or zinc proteases [66, 67]. Also, the expected drug lopinavir/ritonavir has been designed for HIV-protease, which is aspartic protease. These proteases are structurally distinct from 3C-like proteinase known to be a cysteine protease. This observation implies that structure optimizations would likely be required for repurposed drugs for SARS-CoV-2 3C-like proteinase. Consequently, the presented study suggested carfilzomib, which has been targeted toward threonine protease and approved for multiple myeloma treatment [47, 48], as a marginally resembling drug.

The model showed, however, carfilzomib fit well into the active site by forming considerable stabilizing interactions and no severe steric hinderance (Fig. 1C).

Another potential target is the complex of surface glycoprotein and ACE2 to prevent virus entry into the cell [68, 69]. Many hypertension drugs are targeted to ACE, and the presented study highlighted the approved drugs, namely, lisinopril, enalaprila, and captopril, as potential ligands for ACE2. An expectation in advance was to find a drug that bound to ACE2 and also interfered the interactions between surface glycoprotein and ACE2. However, as the models revealed, the drug-binding site of ACE2 existed inside a deep cleft in the center of ACE2 molecule, and the ligands do not interact directly with the surface glycoprotein (Fig. 2C). Also, most of the drugs are targeted toward ACE (not ACE2), and ACE and ACE2 diverge considerably in their amino acid sequences (44% identity). Therefore, effects of the ACE drugs on preventing surface glycoprotein - ACE2 interactions would not be highly promising.

Another target presented results highlighted was 2'-O-ribose methyltransferase (nsp16) – nsp10 complex, which is less focused as a target of drug repurposing. 2'-O-ribose methyltransferase is required to finalize the cap structure, $^{7Me}GpppA_{2'OMe}$, of coronavirus RNAs by transferring a methyl group to 2' OH group of ribonucleotide from S-adenosyl-L-methionine [70, 71]. The cap structure is essential for viral mRNAs to be translated and escape from innate immune system in the host cell. Thus, inhibition of this enzyme might prevent virus propagation. Despite the overall sequence identities between templates (SARS-CoV or Human betacoronavirus) and SARS-CoV-2 enzymes were relatively low (~66%), the residues interacting with the drugs were conserved.

Among the suggested drugs for this enzyme, sinefungin is a naturally occurring and verified inhibitor of 2'-*O*-ribose methyltransferase. Since a toxicity was detected [72], however, appreciation of this natural drug should be carefully considered. Although tecadenoson has been examined in a clinical trial for atrial fibrillation, and passed phase II test, final results were not formally reported at this point of time [73]. Trabodenoson was designed for treating ocular hypertension and primary open-angle glaucoma [74], but had failed in the phase III clinical trial test due to lack of superiority over placebo. Selodenoson was designed to control heart rate [75], and it seems still in a developmental stage. Since tecadenoson and trabodenoson appeared to have cleared the phase I tests, these drugs would worth examining against COVID-19.

Several structure determinations of SARS-CoV-2 proteins, e.g., endoRNase (PDB IDs 6vww and 6vw01) and nucleocapsid phosphoprotein (6vyo), have been reported after the modeling of the presented study have been executed. Although many of the other proteins should be under analyses undoubtedly, it would take considerable time before all structures of potential targets are experimentally elucidated. During the period until the structural determinations, theoretical models might be useful. The presented structural models are freely available from the BINDS webpage (https://www.binds.jp/SARS-CoV-2/) and also deposited in the BSM-Arc repository (BSM00015) [76].

ACKNOWLEDGEMENTS

AUTHOR CONTRIBUTIONS

M.O., S.K., and T.S. conceived and designed the study. A.H., C.S. S.N. M.S. and T.S. constructed the models. A.H., C.S. and T.S. wrote the manuscript. All authors commented on the manuscript.

DECLARATION OF INTERESTS

The authors declare no competing interests.

Table 1. Models of SARS-CoV-2 protein [*1]

Gene	Protein	Name	Length	Model template					Model				
				PDB ID	Identity (%)	Coverage (%)	Model description	Region	Interacting protein	Ligand	Rotamer outlier (%)	Ramachandran outlier (%)	Clash score
orf1ab	YP_009725297.1	Leader protein	180	2hsxA	85.3	66.7	monomer(A)	A: 10 - 129			0.97	0	4.75
	YP_009725298.1	nsp2	638	n.a.									
	YP_009725299.1	Papain-like proteinase (nsp3)	1945	2idyA	79.3	5.9	monomer(A)	A: 1 - 114			0.98	0	4.55
				2favC	72.5	9.2	monomer(A)	A: 202 - 379			0.67	0	4.41
				2wctB	76.3	13.9	homo-dimer(A, B)	A, B: 410 - 679			1.27	0	4.96
				2kqwA	72.7	3.7	monomer(A)	A: 675 - 746			1.52	0	4.41
				5e6jA	82.0	16.6	monomer(A)	A: 745 - 1067			0.35	0	3.71
				2k87A	81.0	6.3	monomer(A)	A: 1085 - 1206			1.79	0	3.58
	YP_009725300.1	nsp4	500	3gzfA	40.0	20.4	homo-dimer(A, B)	A: 399 - 500 B: 399 - 497			1.69	0	3.43
	YP_009725301.1	3C-like proteinase	306	6lu7A	100.0	100.0	homo-dimer(A, C)	A, C: 1 - 306		AZP, Carfilzomib	0	0	4.54
	YP_009725302.1	nsp6	290	n.a.									
	YP_009725303.1	nsp7	83	2kysA	98.8	100.0	monomer(A)	A: 1 - 83			1.3	0	4.57
	YP_009725304.1	nsp8	198	2ahmH	97.4	98.5	hetero-16mer(E, F, G, H, S, T, U, V)	E, S: 35 - 195 F, T: 47 - 195 G, U: 1 - 194 H, V: 1 - 195	nsp7 (A, B, C, D, O, P, Q, R)		1.08	0	4.42
	YP_009725305.1	nsp9	113	1uw7A	97.3	100.0	homo-dimer(A, B)	A, B: 1 - 113			1.6	0	4.86
	YP_009725306.1	nsp10	139	5nfyH	98.5	96.4	hetero-dimer(B)	B: 1 - 134	3'-to-5' exonuclease (A)	ZN	1.23	0	4.78
	YP_009725307.1	RNA-dependent RNA polymerase	932	6nurA	96.3	86.8	hetero-tetramer(A)	A: 114 - 922	nsp8 (B, D), nsp7(C)	ZN	0.81	0	4.87
	YP_009725308.1	Helicase	601	5wwpA	71.5	99.7	monomer(A)	A: 1 - 599		ZN	1.54	0	4.82
	YP_009725309.1	3'-to-5' Exonuclease	527	5nfyD	94.7	100.0	hetero-dimer(A)	A: 1 - 527	nsp10 (B)	ZN	1.23	0	4.78
	YP_009725310.1	Endo-RNAse	346	2h85A	88.1	100.0	homo-hexamer(A, B, C, D, E, F)	A, B, C, D, E, F: 1 - 346			0.92	0	4.75
	YP_009725311.1	2'-O-Ribose methyltransferase	298	5yniA	66.3	100.0	hetero-dimer(A)	A: 1-298	nsp10 (B)	GTG, ZN, Sinefungin	1.66	0	4.69
										GTG, ZN, Tecadenoson			4.86
										GTG, ZN, Selodenoson			4.55
										GTG, ZN, Trabodenoson			4.40
	YP_009725312.1	nsp11	13	n.a.									

Table 1. *Continued*

Protein	RefSeq ID	Model description	Length	PDB ID	Identity	Coverage	Model description	Region	Interacting protein	Ligand	Rotamer outlier	Ramachandran outlier	Clash score
S	YP_009724390.1	Surface glycoprotein	1273	6vsbA	100.0	88.6	homo-trimer(A, B, C)	A, B, C: 13 - 1140	ACE2 (D)	EAL	1.63	0.08	5.83
										LPR			5.86
										X8Z			5.86
ORF3a	YP_009724391.1	ORF3a protein	275	n.a.									
E	YP_009724392.1	Envelope protein	75	5x29E	91.4	90.7	homo-pentamer(A, B, C, D, E)	A, C, D, E: 5 - 68 B: 1 - 68			1.67	0	4.63
M	YP_009724393.1	Membrane glycoprotein	222	n.a.									
ORF6	YP_009724394.1	ORF6 protein	61	n.a.									
ORF7a	YP_009724395.1	ORF7a protein	121	1yo4A	88.4	75.2	monomer(A)	A: 11 - 101			0	0	4.92
ORF7b	YP_009725296.1	ORF7b	43	n.a.									
ORF8	YP_009724396.1	ORF8 protein	121	n.a.									
N	YP_009724397.2	Nucleocapsid phosphoprotein	419	1sskA	81.6	39.1	monomer(A)	A: 20 - 183			1.56	0	4.88
				2jw8B	95.8	30.1	homo-dimer(A, B)	A: 243 - 367 B: 242 - 367			0.48	0	3.31
ORF10	YP_009725255.1	ORF10 protein	38	n.a.									

*1 "Protein" indicates Refseq IDs of SARS-CoV-2 proteins, and also serves as the model identifiers. "Model template": "Identity" and "Coverage" show amino acid sequence identity and coverage of the template structure ("PDB ID") to the corresponding SARS-CoV-2 proteins. "Model": "Model description" and "Interacting protein" show chain ID(s) of the corresponding and bounding proteins, respectively. "Region" shows chain ID(s) and the start and end residue numbers of modeled region. "Ligand" shows the names or PDB codes of ligands in the template or models structures. "Rotamer outlier", "Ramachandran outlier", and "Clash score" show the parameters of the models.

Table 2. Potential drugs for SARS-CoV-2 [*1]

Ligand name	Ligand code	Protein name	Protein sources	PDB IDs	Score	Drug name	DB codes
S-adenosyl-L-methionine	SAM	2'-*O*-Ribose methyl transferase (nsp16)	SARS-CoV, Human betacoronavirus 2C EMC/2012	5c8t, 3r24, 5yni, 5ynm, 5yn6	1.000	Ademetionine	D07128
					0.946	Sinefungin	C00052045, D05846
					0.862	Tecadenoson	D06019
					0.814	Selodenoson	D05818
					0.814	Trabodenoson	D10493
Sinefungin	SFG	2'-*O*-Ribose methyl transferase (nsp16)	SARS-CoV, Human betacoronavirus 2C EMC/2012	2xyr, 5ynn, 5ynp, 5ynb	1.000	Sinefungin	C00052045, D05846
					0.946	Ademetionine	D07128
					0.862	Tecadenoson	D06019
					0.832	Adenosine monophosphate	D02769
					0.832	Selodenoson	D05818
7-Methyl-Guanosine-5'-Triphosphte-5'-Guanosine	GTG	2'-*O*-Ribose methyl transferase	Human betacoronavirus 2C EMC/2012	5yni, 5ynn	0.788	Nadide	D00002
					0.763	Diquafosol tetrasodium	D03864
Ace-Ser-Ala-Val-ALC-His-H	n.a	3C-like proteinase	SARS-CoV	3avz	n.d.		
N-[(5-methylisoxazol-3-yl)carbonyl]alanyl-L-valyl-N~1-((1R,2Z)-4-(benzyloxy)-4-oxo-1-{[(3R)-2-oxopyrrolidin-3-yl]methyl}but-2-enyl)-L-leucinamide	n.a	3C-like proteinase	SARS-CoV-2	6lu7	n.d.		
C4Z inhibitor	n.a	3C-like proteinase	SARS-CoV	3vb5	n.d.		

17

Table 2. *Continued*

Ac-ESTLQ-H	n.a	3C-like proteinase	SARS-CoV	3snd	0.783	Magnesium pidolate	D08263	
					0.779	Decanal	C00030099	
					0.779	1-Decanol	C00030100	
					0.775	Undecanal	C00032442	
(5s,8s,14r)-Ethyl 11-(3-Amino-3-Oxopropyl)-8-Benzyl-14-Hydroxy-5-Isobutyl-3,6,9,12-Tetraoxo-1-Phenyl-2-Oxa-4,7,10,11-Tetraazapentadecan-15-Oate	AZP	3C-like proteinase	SARS-CoV	2gtb	0.754	Carfilzomib	D08880	
1-((2S)-2-{[(1S)-1-Carboxy-3-Phenylpropyl]Amino}Propanpyl)-L-Proline	EAL	ACE	Human	1uze	1.000	Enalaprilat	D03769	
					0.932	Lisinopril	D00362	
					0.926	Enalapril	D00621	
					0.925	Spiraprilat	D03775	
					0.918	Lisinopril	D00362	
[*N*2-[(*S*)-1-Carboxy-3-phenylpropyl]-L-lysyl-L-proline	LPR	ACE somatic isoform	Human	1o86	1.000	Lisinopril	D00362	
					0.932	Enalaprilat	D03769	
					0.896	Enalapril	D07892	
					0.867	Ceronapril	D03440	
					0.857	Spiraprilat	D03775	
L-Captopril	X8Z	ACE	Human	4c2p	1.000	Captopril	D00251	
					0.853	Telmesteine	D08565	
					0.851	Oxaceprol	D07215	
					0.795	Undecanoic acid	C00007421	
					0.795	Bucillamine	D01809	

[*1] "Protein source" and "PDB ID" are the source organisms and PDB of the template structures, respectively. "Ligand code" is HETATM code in PDB. "DB code" is headed by D and C for the IDs of the molecules in KEGG and KNApSAcK, respectively.

REFERENCES

1. Wu, F., Zhao, S., Yu, B., Chen, Y.M., Wang, W., Song, Z.G., Hu, Y., Tao, Z.W., Tian, J.H., Pei, Y.Y., et al. (2020). A new coronavirus associated with human respiratory disease in China. Nature.

2. Gralinski, L.E., and Menachery, V.D. (2020). Return of the Coronavirus: 2019-nCoV. Viruses *12*.

3. Lu, H. (2020). Drug treatment options for the 2019-new coronavirus (2019-nCoV). Biosci Trends.

4. Wang, M., Cao, R., Zhang, L., Yang, X., Liu, J., Xu, M., Shi, Z., Hu, Z., Zhong, W., and Xiao, G. (2020). Remdesivir and chloroquine effectively inhibit the recently emerged novel coronavirus (2019-nCoV) in vitro. Cell Res *30*, 269-271.

5. Gao, J., Tian, Z., and Yang, X. (2020). Breakthrough: Chloroquine phosphate has shown apparent efficacy in treatment of COVID-19 associated pneumonia in clinical studies. Biosci Trends.

6. Fan, H.H., Wang, L.Q., Liu, W.L., An, X.P., Liu, Z.D., He, X.Q., Song, L.H., and Tong, Y.G. (2020). Repurposing of clinically approved drugs for treatment of coronavirus disease 2019 in a 2019-novel coronavirus (2019-nCoV) related coronavirus model. Chin Med J (Engl).

7. Dong, L., Hu, S., and Gao, J. (2020). Discovering drugs to treat coronavirus disease 2019 (COVID-19). Drug Discov Ther *14*, 58-60.

8. Wrapp, D., Wang, N., Corbett, K.S., Goldsmith, J.A., Hsieh, C.L., Abiona, O., Graham, B.S., and McLellan, J.S. (2020). Cryo-EM structure of the 2019-nCoV spike in the prefusion conformation. Science.

9. Li, G., and De Clercq, E. (2020). Therapeutic options for the 2019 novel coronavirus (2019-nCoV). Nat Rev Drug Discov *19*, 149-150.

10. Ling, C.Q. (2020). Traditional Chinese medicine is a resource for drug discovery against 2019 novel coronavirus (SARS-CoV-2). J Integr Med.

11. Pang, J., Wang, M.X., Ang, I.Y.H., Tan, S.H.X., Lewis, R.F., Chen, J.I., Gutierrez, R.A., Gwee, S.X.W., Chua, P.E.Y., Yang, Q., et al. (2020). Potential Rapid Diagnostics, Vaccine and Therapeutics for 2019 Novel Coronavirus (2019-nCoV): A Systematic Review. J Clin Med *9*.

12. de Wit, E., van Doremalen, N., Falzarano, D., and Munster, V.J. (2016). SARS and MERS: recent insights into emerging coronaviruses. Nat Rev Microbiol *14*, 523-534.

13. Song, Z., Xu, Y., Bao, L., Zhang, L., Yu, P., Qu, Y., Zhu, H., Zhao, W., Han, Y., and Qin, C. (2019). From SARS to MERS, Thrusting Coronaviruses into the Spotlight. Viruses *11*.

14. Chan, K.S., Lai, S.T., Chu, C.M., Tsui, E., Tam, C.Y., Wong, M.M., Tse, M.W., Que, T.L., Peiris, J.S., Sung, J., et al. (2003). Treatment of severe acute respiratory syndrome with lopinavir/ritonavir: a multicentre retrospective matched cohort study. Hong Kong Med J *9*, 399-406.

15. Chu, C.M., Cheng, V.C., Hung, I.F., Wong, M.M., Chan, K.H., Chan, K.S., Kao, R.Y., Poon, L.L., Wong, C.L., Guan, Y., et al. (2004). Role of lopinavir/ritonavir in the treatment of SARS: initial virological and clinical findings. Thorax *59*, 252-256.

16. Nguyen, D.D., Gao, K., Chen, J., Wang, R., and Wei, G.-W. (2020). Potentially highly potent drugs for 2019-nCoV. bioRxiv, 2020.2002.2005.936013.

17. Xu, Z., Peng, C., Shi, Y., Zhu, Z., Mu, K., Wang, X., and Zhu, W. (2020). Nelfinavir was predicted to be a potential inhibitor of 2019-nCov main protease by an integrative approach combining homology modelling, molecular docking and binding free energy calculation. bioRxiv, 2020.2001.2027.921627.

18. Alex, Z., Vladimir, A., Alexander, Z., Bogdan, Z., Victor, T., Dmitry S., B., Daniil, P., Rim, S., Andrey, F., Philipp, O., et al. (2020). Potential COVID-2019 3C-like Protease Inhibitors Designed Using Generative Deep Learning Approaches.

19. Gordon, C.J., Tchesnokov, E.P., Feng, J.Y., Porter, D.P., and Gotte, M. (2020). The antiviral compound remdesivir potently inhibits RNA-dependent RNA polymerase from Middle East respiratory syndrome coronavirus. J Biol Chem.

20. Ashburn, T.T., and Thor, K.B. (2004). Drug repositioning: identifying and developing new uses for existing drugs. Nat Rev Drug Discov *3*, 673-683.

21. Yildirim, M.A., Goh, K.I., Cusick, M.E., Barabasi, A.L., and Vidal, M. (2007). Drug-target network. Nat Biotechnol *25*, 1119-1126.

22. Menche, J., Sharma, A., Kitsak, M., Ghiassian, S.D., Vidal, M., Loscalzo, J., and Barabasi, A.L. (2015). Disease networks. Uncovering disease-disease relationships through the incomplete interactome. Science *347*, 1257601.

23. Li, J., Zheng, S., Chen, B., Butte, A.J., Swamidass, S.J., and Lu, Z. (2016). A survey of current trends in computational drug repositioning. Brief Bioinform *17*, 2-12.

24. Pushpakom, S., Iorio, F., Eyers, P.A., Escott, K.J., Hopper, S., Wells, A., Doig, A., Guilliams, T., Latimer, J., McNamee, C., et al. (2019). Drug repurposing: progress, challenges and recommendations. Nat Rev Drug Discov *18*, 41-58.

25. Masoudi-Sobhanzadeh, Y., Omidi, Y., Amanlou, M., and Masoudi-Nejad, A. (2020). Drug databases and their contributions to drug repurposing. Genomics *112*, 1087-1095.

26. Zhang, L., Lin, D., Sun, X., Curth, U., Drosten, C., Sauerhering, L., Becker, S., Rox, K., and Hilgenfeld, R. (2020). Crystal structure of SARS-CoV-2 main protease provides a basis for design of improved α-ketoamide inhibitors. Science, eabb3405.

27. O'Leary, N.A., Wright, M.W., Brister, J.R., Ciufo, S., Haddad, D., McVeigh, R., Rajput, B., Robbertse, B., Smith-White, B., Ako-Adjei, D., et al. (2016). Reference sequence (RefSeq) database at NCBI: current status, taxonomic expansion, and functional annotation. Nucleic Acids Res *44*, D733-745.

28. Berman, H., Henrick, K., and Nakamura, H. (2003). Announcing the worldwide Protein Data Bank. Nat Struct Biol *10*, 980.

29. Altschul, S.F., Gish, W., Miller, W., Myers, E.W., and Lipman, D.J. (1990). Basic local alignment search tool. J Mol Biol *215*, 403-410.

30. Webb, B., and Sali, A. (2014). Comparative Protein Structure Modeling Using MODELLER. Curr Protoc Bioinformatics *47*, 5 6 1-5 6 32.

31. Adams, P.D., Afonine, P.V., Bunkoczi, G., Chen, V.B., Davis, I.W., Echols, N., Headd, J.J., Hung, L.W., Kapral, G.J., Grosse-Kunstleve, R.W., et al. (2010). PHENIX: a comprehensive Python-based system for macromolecular structure solution. Acta Crystallogr D Biol Crystallogr *66*, 213-221.

32. Emsley, P., Lohkamp, B., Scott, W.G., and Cowtan, K. (2010). Features and development of Coot. Acta Crystallogr D Biol Crystallogr *66*, 486-501.

33. Williams, C.J., Headd, J.J., Moriarty, N.W., Prisant, M.G., Videau, L.L., Deis, L.N., Verma, V., Keedy, D.A., Hintze, B.J., Chen, V.B., et al. (2017). MolProbity: More and better reference data for improved all-atom structure validation. Protein Sci.

34. Kanehisa, M., Goto, S., Sato, Y., Furumichi, M., and Tanabe, M. (2012). KEGG for integration and interpretation of large-scale molecular data sets. Nucleic Acids Res *40*, D109-114.

35. Wishart, D.S., Feunang, Y.D., Guo, A.C., Lo, E.J., Marcu, A., Grant, J.R., Sajed, T., Johnson, D., Li, C., Sayeeda, Z., et al. (2018). DrugBank 5.0: a major update to the DrugBank database for 2018. Nucleic Acids Res *46*, D1074-D1082.

36. Afendi, F.M., Okada, T., Yamazaki, M., Hirai-Morita, A., Nakamura, Y., Nakamura, K., Ikeda, S., Takahashi, H., Altaf-Ul-Amin, M., Darusman, L.K., et al. (2012). KNApSAcK family databases: integrated metabolite-plant species databases for multifaceted plant research. Plant Cell Physiol *53*, e1.

37. Saito, M., Takemura, N., and Shirai, T. (2012). Classification of ligand molecules in PDB with fast heuristic graph match¥ algorithm COMPLIG. J Mol Biol *424*, 379-390.

38. Weiss, S.R., Hughes, S.A., Bonilla, P.J., Turner, J.D., Leibowitz, J.L., and Denison, M.R. (1994). Coronavirus polyprotein processing. Arch Virol Suppl *9*, 349-358.

39. Hirokawa, T., Boon-Chieng, S., and Mitaku, S. (1998). SOSUI: classification and secondary structure prediction system for membrane proteins. Bioinformatics *14*, 378-379.

40. Dias, D.A., Urban, S., and Roessner, U. (2012). A historical overview of natural products in drug discovery. Metabolites *2*, 303-336.

41. Mushtaq, S., Abbasi, B.H., Uzair, B., and Abbasi, R. (2018). Natural products as reservoirs of novel therapeutic agents. EXCLI J *17*, 420-451.

42. Thiel, V., Ivanov, K.A., Putics, A., Hertzig, T., Schelle, B., Bayer, S., Weissbrich, B., Snijder, E.J., Rabenau, H., Doerr, H.W., et al. (2003). Mechanisms and enzymes involved in SARS coronavirus genome expression. J Gen Virol *84*, 2305-2315.

43. Lee, T.W., Cherney, M.M., Liu, J., James, K.E., Powers, J.C., Eltis, L.D., and James, M.N. (2007). Crystal structures reveal an induced-fit binding of a substrate-like Aza-peptide epoxide to SARS coronavirus main peptidase. J Mol Biol *366*, 916-932.

44. Akaji, K., Konno, H., Mitsui, H., Teruya, K., Shimamoto, Y., Hattori, Y., Ozaki, T., Kusunoki, M., and Sanjoh, A. (2011). Structure-based design, synthesis, and evaluation of peptide-mimetic SARS 3CL protease inhibitors. J Med Chem *54*, 7962-7973.

45. Zhu, L., George, S., Schmidt, M.F., Al-Gharabli, S.I., Rademann, J., and Hilgenfeld, R. (2011). Peptide aldehyde inhibitors challenge the substrate specificity of the SARS-coronavirus main protease. Antiviral Res *92*, 204-212.

46. Chuck, C.P., Chen, C., Ke, Z., Wan, D.C., Chow, H.F., and Wong, K.B. (2013). Design, synthesis and crystallographic analysis of nitrile-based broad-spectrum peptidomimetic inhibitors for coronavirus 3C-like proteases. Eur J Med Chem *59*, 1-6.

47. Kuhn, D.J., Chen, Q., Voorhees, P.M., Strader, J.S., Shenk, K.D., Sun, C.M., Demo, S.D., Bennett, M.K., van Leeuwen, F.W., Chanan-Khan, A.A., et al. (2007). Potent activity of carfilzomib, a novel, irreversible inhibitor of the ubiquitin-proteasome pathway, against preclinical models of multiple myeloma. Blood *110*, 3281-3290.

48. Kortuem, K.M., and Stewart, A.K. (2013). Carfilzomib. Blood *121*, 893-897.

49. Goetz, D.H., Choe, Y., Hansell, E., Chen, Y.T., McDowell, M., Jonsson, C.B., Roush, W.R., McKerrow, J., and Craik, C.S. (2007). Substrate specificity profiling and identification of a new class of inhibitor for the major protease of the SARS coronavirus. Biochemistry *46*, 8744-8752.

50. Li, W., Moore, M.J., Vasilieva, N., Sui, J., Wong, S.K., Berne, M.A., Somasundaran, M., Sullivan, J.L., Luzuriaga, K., Greenough, T.C., et al. (2003). Angiotensin-converting enzyme 2 is a functional receptor for the SARS coronavirus. Nature *426*, 450-454.

51. Natesh, R., Schwager, S.L., Sturrock, E.D., and Acharya, K.R. (2003). Crystal structure of the human angiotensin-converting enzyme-lisinopril complex. Nature *421*, 551-554.

52. Natesh, R., Schwager, S.L., Evans, H.R., Sturrock, E.D., and Acharya, K.R. (2004). Structural details on the binding of antihypertensive drugs captopril and enalaprilat to human testicular angiotensin I-converting enzyme. Biochemistry *43*, 8718-8724.

53. Yates, C.J., Masuyer, G., Schwager, S.L., Akif, M., Sturrock, E.D., and Acharya, K.R. (2014). Molecular and thermodynamic mechanisms of the chloride-dependent human angiotensin-I-converting enzyme (ACE). J Biol Chem *289*, 1798-1814.

54. Brunner, H.R., Waeber, B., Wauters, J.P., Turin, G., McKinstry, D., and Gavras, H. (1978). Innappropriate renin secretion unmasked by captopril (SQ 14 225) in hypertension of chronic renal failure. Lancet *2*, 704-707.

55. Gross, D.M., Sweet, C.S., Ulm, E.H., Backlund, E.P., Morris, A.A., Weitz, D., Bohn, D.L., Wenger, H.C., Vassil, T.C., and Stone, C.A. (1981). Effect of N-[(S)-1-carboxy-3-phenylpropyl]-L-Ala-L-Pro and its ethyl ester (MK-421) on angiotensin converting enzyme in vitro and angiotensin I pressor responses in vivo. J Pharmacol Exp Ther *216*, 552-557.

56. Brunner, D.B., Desponds, G., Biollaz, J., Keller, I., Ferber, F., Gavras, H., Brunner, H.R., and Schelling, J.L. (1981). Effect of a new angiotensin converting enzyme inhibitor MK 421 and its lysine analogue on the components of the renin system in healthy subjects. Br J Clin Pharmacol *11*, 461-467.

57. Ondetti, M.A. (1994). From peptides to peptidases: a chronicle of drug discovery. Annu Rev Pharmacol Toxicol *34*, 1-16.

58. Chen, Y., Cai, H., Pan, J., Xiang, N., Tien, P., Ahola, T., and Guo, D. (2009). Functional screen reveals SARS coronavirus nonstructural protein nsp14 as a novel cap N7 methyltransferase. Proc Natl Acad Sci U S A *106*, 3484-3489.

59. Chen, Y., Su, C., Ke, M., Jin, X., Xu, L., Zhang, Z., Wu, A., Sun, Y., Yang, Z., Tien, P., et al. (2011). Biochemical and structural insights into the mechanisms of SARS coronavirus RNA ribose 2'-O-methylation by nsp16/nsp10 protein complex. PLoS Pathog *7*, e1002294.

60. Decroly, E., Debarnot, C., Ferron, F., Bouvet, M., Coutard, B., Imbert, I., Gluais, L., Papageorgiou, N., Sharff, A., Bricogne, G., et al. (2011). Crystal structure

and functional analysis of the SARS-coronavirus RNA cap 2'-O-methyltransferase nsp10/nsp16 complex. PLoS Pathog *7*, e1002059.

61. Ma, Y., Wu, L., Shaw, N., Gao, Y., Wang, J., Sun, Y., Lou, Z., Yan, L., Zhang, R., and Rao, Z. (2015). Structural basis and functional analysis of the SARS coronavirus nsp14-nsp10 complex. Proc Natl Acad Sci U S A *112*, 9436-9441.

62. Sharma, A., Gerbarg, P., Bottiglieri, T., Massoumi, L., Carpenter, L.L., Lavretsky, H., Muskin, P.R., Brown, R.P., Mischoulon, D., and as Work Group of the American Psychiatric Association Council on, R. (2017). S-Adenosylmethionine (SAMe) for Neuropsychiatric Disorders: A Clinician-Oriented Review of Research. J Clin Psychiatry *78*, e656-e667.

63. Robert-Géro, M., Lawrence, F., Blanchard, P., Dodic, N., Paolantonacci, P., and Malina, H. (1989). Antileishmanial Effect of Sinefungin and its Derivatives. . In Leishmaniasis. NATO ASI Series (Series A: Life Sciences), Volume 171, D.T. Hart, ed. (Boston: Springer).

64. McCarthy, M.W., and Walsh, T.J. (2018). Amino Acid Metabolism and Transport Mechanisms as Potential Antifungal Targets. Int J Mol Sci *19*.

65. Kuroda, Y., Yamagata, H., Nemoto, M., Inagaki, K., Tamura, T., and Maeda, K. (2019). Antiviral effect of sinefungin on in vitro growth of feline herpesvirus type 1. J Antibiot (Tokyo) *72*, 981-985.

66. Hopkins, A.L., and Groom, C.R. (2002). The druggable genome. Nat Rev Drug Discov *1*, 727-730.

67. Wang, J., Yazdani, S., Han, A., and Schapira, M. (2020). Structure-based view of the druggable genome. Drug Discov Today.

68. Zhang, H., Penninger, J.M., Li, Y., Zhong, N., and Slutsky, A.S. (2020). Angiotensin-converting enzyme 2 (ACE2) as a SARS-CoV-2 receptor: molecular mechanisms and potential therapeutic target. Intensive Care Medicine.

69. Hoffmann, M., Kleine-Weber, H., Schroeder, S., Kruger, N., Herrler, T., Erichsen, S., Schiergens, T.S., Herrler, G., Wu, N.H., Nitsche, A., et al. (2020). SARS-CoV-2 Cell Entry Depends on ACE2 and TMPRSS2 and Is Blocked by a Clinically Proven Protease Inhibitor. Cell.

70. Bouvet, M., Debarnot, C., Imbert, I., Selisko, B., Snijder, E.J., Canard, B., and Decroly, E. (2010). In vitro reconstitution of SARS-coronavirus mRNA cap methylation. PLoS Pathog *6*, e1000863.

71. Chen, Y., and Guo, D. (2016). Molecular mechanisms of coronavirus RNA capping and methylation. Virol Sin *31*, 3-11.

72. Hamil, R.L., and Hoehn, M.M. (1973). A9145, a new adenine-containing antifungal antibiotic. I. Discovery and isolation. J Antibiot (Tokyo) *26*, 463-465.

73. Peterman, C., and Sanoski, C.A. (2005). Tecadenoson: a novel, selective A1 adenosine receptor agonist. Cardiol Rev *13*, 315-321.

74. Li, G., Torrejon, K.Y., Unser, A.M., Ahmed, F., Navarro, I.D., Baumgartner, R.A., Albers, D.S., and Stamer, W.D. (2018). Trabodenoson, an Adenosine Mimetic With A1 Receptor Selectivity Lowers Intraocular Pressure by Increasing Conventional Outflow Facility in Mice. Invest Ophthalmol Vis Sci *59*, 383-392.

75. Savelieva, I., and Camm, J. (2008). Anti-arrhythmic drug therapy for atrial fibrillation: current anti-arrhythmic drugs, investigational agents, and innovative approaches. Europace *10*, 647-665.

76. Bekker, G.J., Kawabata, T., and Kurisu, G. (2020). The Biological Structure Model Archive (BSM-Arc): an archive for in silico models and simulations. Biophys Rev.
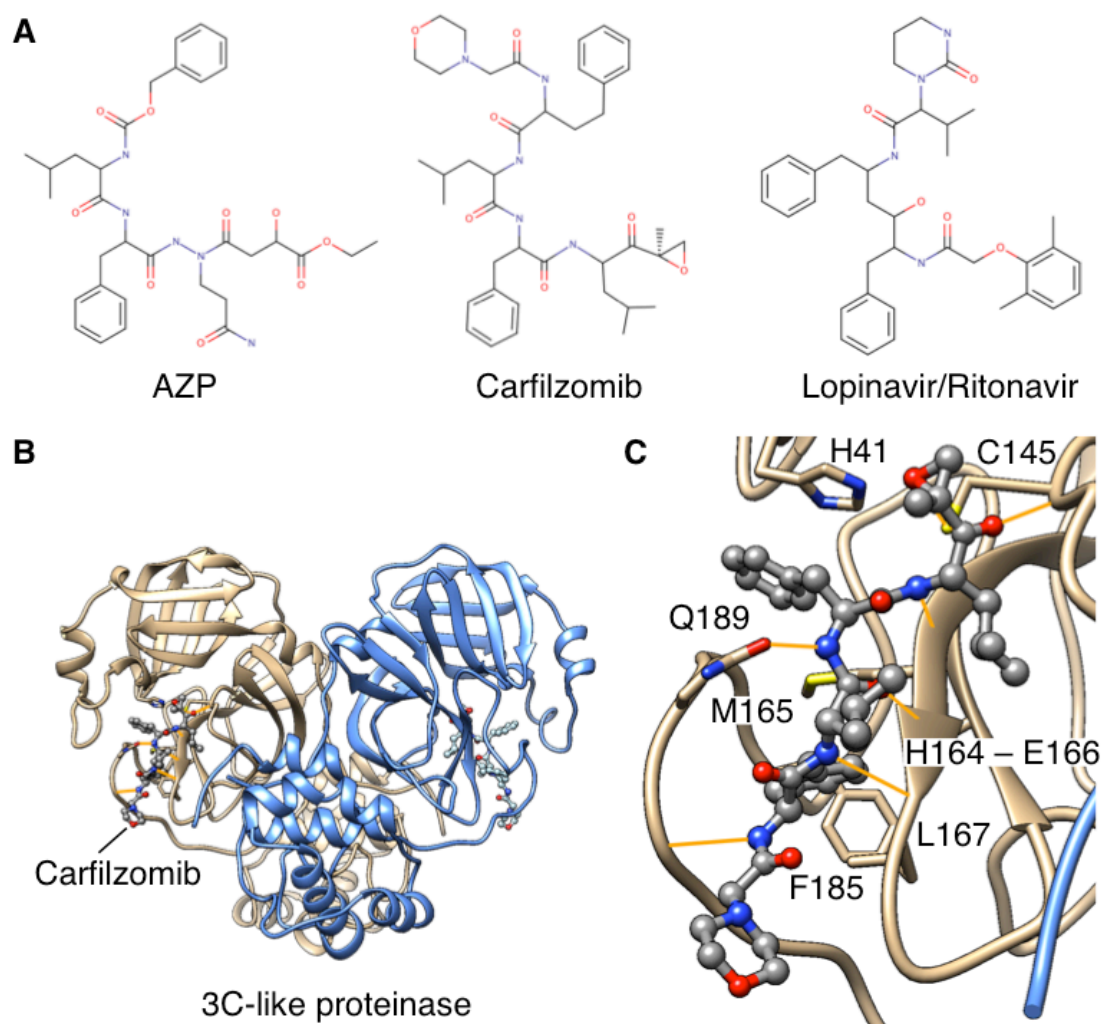
Figure 1. 3C-like proteinase – carfilzomib model

(A) Formula of (5s, 8s, 14r)-ethyl 11-(3-amino-3-oxopropyl)-8-benzyl-14-hydroxy-5-isobutyl-3, 6, 9, 12-tetraoxo-1-phenyl-2-oxa-4, 7, 10, 11-tetraazapentadecan-15-oate (template ligand with ligand code AZP), carfilzomib, and lopinavir/ritonavir. (B) Overall structure of the model. (C) Close view of the carfilzomib binding-site. Hydrogen-bonds are shown in yellow lines.
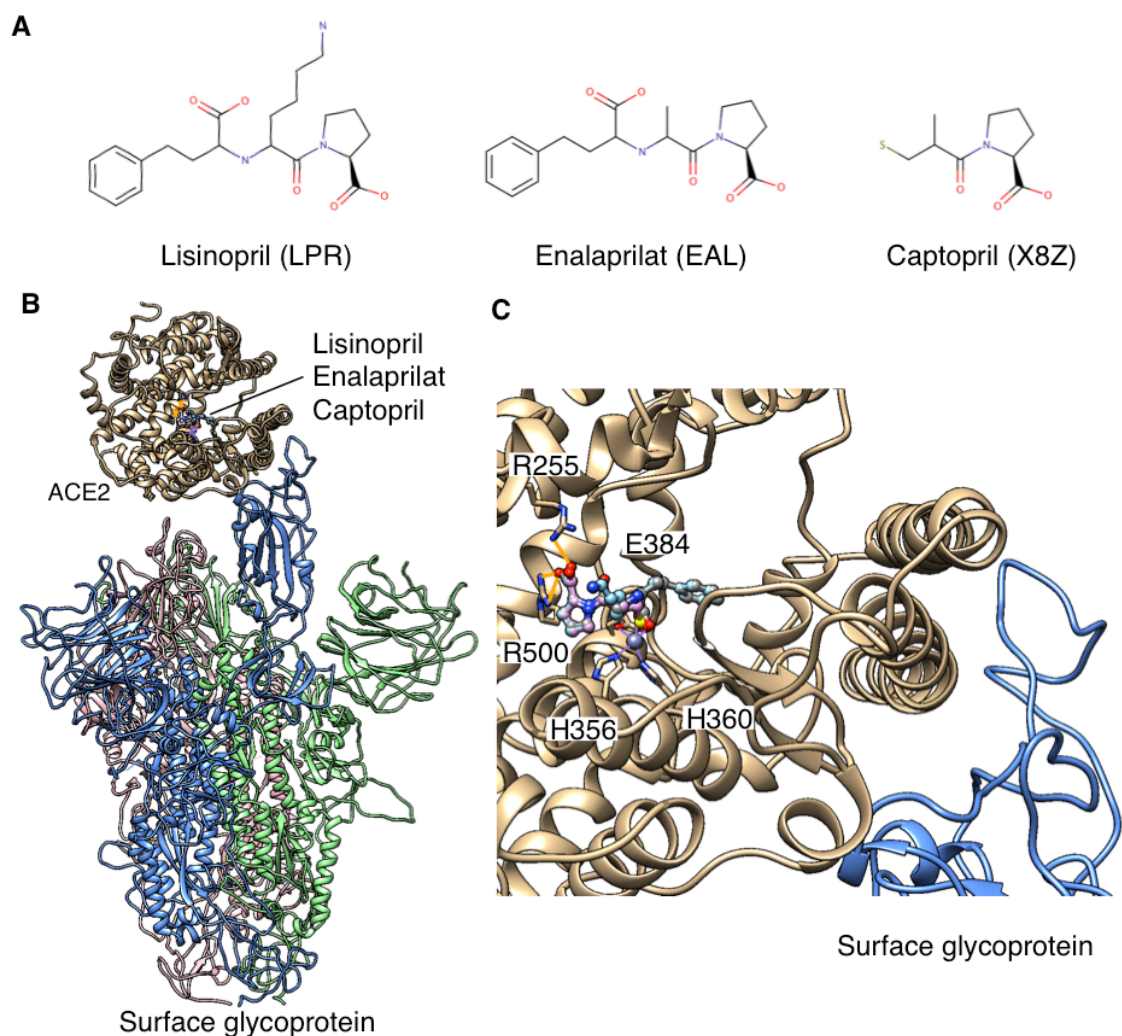
Figure 2. Surface glycoprotein – ACE2 – lisinopril/enalaprilat/captopril model

(A) Formula of lisinopril (ligand code LPR), enalaprilat (EAL), and captopril (X8Z).

(B) Overall structure of the model. (C) Close view of the lisinopril/enalaprilat/captopril

binding-site. Hydrogen-bonds are shown in yellow lines. Lisinopril, enalaprilat, and

captopril were superposed and the carbon-atoms were colored light-blue, gray, and
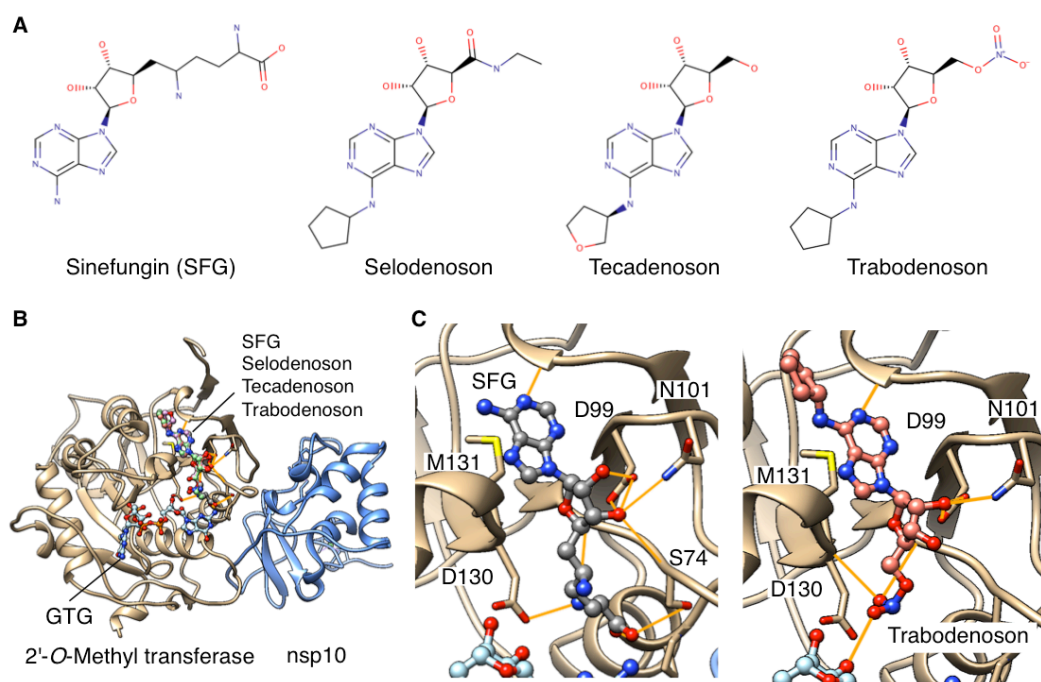
magenta, respectively.

Figure 3. 2'-*O*-Ribose methyltransferase (nsp16) – nsp10 – sinefungin/tecadenoson/ selodenoson/trabodenoson model

(A) Formula of sinefungin (ligand code SFG), tecadenoson, selodenoson, and trabodenoson. (B) Overall structure of the model. (C) Close view of the binding-site for sinefungin (SFG) and trabodenoson. Hydrogen-bonds are shown in yellow lines.